Catalysis of Polymer-Protected Ni/Pd Bimetallic Nano-Clusters for Hydrogenation of Nitrobenzene Derivatives

Ping Lu and Naoki Toshima*,†

Department of Applied Chemistry, School of Engineering, The University of Tokyo, Hongo, Bunkyo-ku, Tokyo 113-8656

†Department of Materials Science and Engineering, Science University of Tokyo in Yamaguchi, Onoda-shi, Yamaguchi 756-0884

(Received July 26, 1999)

Poly(*N*-vinyl-2-pyrrolidone)-protected Ni/Pd bimetallic colloidal nanoparticles, prepared by the polyol reduction method, have been proved to have a nanometer-sized alloy structure with both metals at zerovalent state by our previous study of TEM, XRD, EXAFS, and XPS analyses. Here, dispersions of these bimetallic nanoclusters with different composition ratios are extensively examined as catalysts for the hydrogenation of various nitrobenzene derivatives: i.e., *p*-nitrotoluene, *p*-nitroanisole, 1-nitronaphthalene, *p*-nitrobenzonitrile, and methyl *p*-nitrobenzoate, at 30 °C under an atmospheric pressure of hydrogen. These bimetallic nanoclusters exhibit excellent catalytic properties for the reduction of a nitro group to an amino group with high selectivity. The catalytic activity strongly depends on the metal composition of the particles. The maximum catalytic activity can be observed at a certain intermediate composition ratio, being 3—4 times greater than that of a monometallic colloidal Pd catalyst. A bimetallic nanocluster with the mole ratio of Ni : Pd = 1/4 was the most active catalyst for the hydrogenation of *para*-substituted nitrobenzenes. An approximately linear relationship exists between the hydrogenation rate of the substrate with an electron-donating or electron-withdrawing group and the corresponding Hammett constant of the substituent, as well as between the hydrogenation rate and the LUMO energy level of the substrate.

Nanostructured metal clusters and colloids bridge the gap between their atomic states and bulk states,[1,2] and serve as functional components for materials with diverse electronic, optical, or magnetic properties. They can also act as high performance catalysts for organic and inorganic reactions. Quite a few of these particles have already been shown to have novel catalytic properties, and the applications to catalysis, photocatalysis, and electrocatalysis are rapidly expanding.[3,4]

In recent years, we have achieved good control of the size and structure of the colloidal dispersions of polymer-protected bimetallic nanoclusters in extraordinarily small sizes (from 1 to 3 nm) and narrow size distributions,[5—8] so that the catalytic properties of metal catalysts can be improved by the second element. The bimetallic nanoclusters prepared by simultaneous reduction of two kinds of metal ions by alcohol in the presence of poly(*N*-vinyl-2-pyrrolidone) (PVP) demonstrate superb stability.[9,10] The Pd/Pt and Au/Pd nanoclusters started from $HAuCl_4$, H_2PtCl_6, and $PdCl_2$ are efficient catalysts for selective partial hydrogenation of 1,3-cyclooctadiene to cyclooctene.[11,12] Likewise, Au/Pt[13] and Pt/Rh[14] are also excellent catalysts for visible-light-induced hydrogen evolution.

Although reduction of the late transition metal ions is much more difficult than that of noble metal ions, we have managed to develop a novel method for the preparation of colloidal dispersions of PVP-protected Cu/Pd and Ni/Pd alloy nanoclusters by reducing the corresponding hydroxide precursors with ethylene glycol.[15] This cold alloying method is of universal significance for the preparation of other bimetallic nanoclusters composed of a noble metal and a late transition metal.[16] The alloy structure of the Cu/Pd bimetallic nanoclusters, proved by TEM, XRD, EXAFS, and XPS analyses, has provided a new type of catalyst, which is effective both for the selective hydration of acrylonitrile to acrylamide and for the selective partial hydrogenation of 1,3-cyclooctadiene to cyclooctene.[15] Similarly, the Ni/Pd colloidal dispersions also exhibited definite monodisperse size-distributions, with each particle containing both nickel and palladium atoms.[16,17] Subsequent structural analysis work of Ni/Pd nanoclusters by XRD, EXAFS, and XPS further showed the alloy structure where both atoms appear on the surface of the nanoparticles with zerovalent state. Preliminary investigations have revealed that Ni/Pd nanoclusters can display excellent catalytic performance for hydrogenation of nitrobenzene under an atmospheric pressure.[17] Therefore, the very high catalytic activity of the bimetallic nanoclusters can be understood by an *ensemble* effect.

As is known, the hydrogenation of nitroaromatics by metal catalysts is a reaction of great importance in industry to produce aromatic amines. In fact, aniline can be produced in industries by reduction of nitrobenzene with hydrogen over Cu, Ni, or Pt catalyst or with iron powder and hydrochloric acid according to the classical method, although a novel Dow method uses chlorobenzene and ammonia as the raw materials. Many investigations have already been carried out on supported catalysts: e.g., (a) Cu powders,[18] (b) Cr_2O_3–CuO

supported on MgF_2,[19] and Cu–Cr–Mo supported on silica,[20] (c) Pt or Pd supported on alumina,[21,22] activated carbon, aluminum borate, some copolymers,[23—29] and SiO_2,[30] (d) Ru,[31,32] (e) Rh,[28] (f) Pd(II)[29,33—35] or Pd(II)/Ru(III),[34] Pd/Pt(4/1) on polymers,[34] and (g) PdGe supported on carbon.[36] Most of the previous studies are concerned with the catalysis of single metals, the effect of the supporting materials on the metal, and the modification of supports. The hydrogenation of nitroaromatics by bimetallic catalysts has been investigated in the systems like Pd/Pt,[34] Pd/Ge,[36] Ru/Sn, Ru/Pb, and Ru/Ge.[31] However, little information is available about the substrate activation and the reaction mechanism on bimetallic catalysts. An extensive study of this reaction over bimetallic nanoparticles within a *quantum-size* region is important to fully understand not only the variables in this reaction, but also the effect of bimetallization on the nanoparticle properties. Generally, bimetallic alloy catalysts[37—39] have been found to be superior to single metals in many cases in regard to activity, selectivity and stability in certain types of reactions.[40—46] The catalytic activity of an alloy is not only determined by the electronic structure of an alloy crystal as a whole, but also by localized properties of surface sites. Bimetallic alloys which include a combination of two metals of different groups in the periodic table, e.g., Pd and Cu, have been studied using reactions such as hydrogenolysis,[47] CO oxidation,[48] and CO hydrogenation.[49] In the hydrogenolysis reaction, the group 11 metals, like Cu, act mainly as a diluent of the active component.[50] In the CO oxidation[48] and hydrogenation reactions,[51,52] Cu can act as an active part or behave as a promoter by itself. The interesting activity improvement in alloy catalysts is often a fundamental question to be addressed, albeit the role of each component may be case-specific.

The present work involves an extensive study of the catalytic behavior of the novel type of bimetallic nanoclusters, i.e., PVP-protected Ni/Pd alloy nanoclusters, for the hydrogenation of nitroaromatics. In order to elucidate the substituent effect and the reaction mechanism, various types of nitrobenzene derivatives are compared. The influence of the bimetallization on the activity of the substrates is also illustrated for a better understanding of the bimetallic catalyst performance.

Experimental

Materials and Preparation of the Colloidal Dispersions of Nickel/Palladium Bimetallic Nanoclusters. Poly(*N*-vinyl-2-pyrrolidone) (PVP, K-30, average molecular weight 40000) was purchased from Tokyo Kasei. Co., Ltd. Other reagents, such as nickel sulfate ($NiSO_4 \cdot 7H_2O$), palladium(II) acetate ($Pd(Ac)_2$), dioxane, sodium hydroxide, ethylene glycol, Raney nickel precursor, palladium black, nitrobenzene, *p*-nitroanisole, *p*-nitrotoluene, *p*-chloronitrobenzene, *p*-bromonitrobenzene, *p*-nitrobenzonitrile, methyl *p*-nitrobenzoate, and 1-nitronaphthalene, each having a purity level higher than GR grade, were used without further purification.

The colloidal dispersions of the Ni/Pd bimetallic nanoclusters protected by polymers were prepared by an improved polyol reduction method, as described previously.[17] Briefly, two metal ions were mixed in ethylene glycol at designated mole ratios and the total amount of the metal ions was always kept constant at 2.5 mmol. The solutions were stirred and refluxed at 198 °C for 3 h with a nitrogen flow passing through the reaction system to take away water by-product. The color of the mixed solution suddenly changed from clear yellow to transparent dark brown at an initial stage of the refluxing. The final colloidal dispersion appeared as a transparent dark-brown solution and was rather stable for months under nitrogen at room temperature. PVP-protected monometallic nickel and palladium colloidal dispersions were also obtained by the similar procedure. The nanoclusters were separated from ethylene glycol by vacuum evaporation under reduced pressure of nitrogen with a big freezing trap, and dried under vacuum. W-6 Raney nickel catalysts were prepared in the conventional method, as reported in the references.[53,54]

Hydrogenation of Nitrobenzene and its Derivatives Catalyzed by the Colloidal Dispersion of the Bimetallic Nanoclusters. The hydrogenation of nitrobenzene and its derivatives was carried out in ethanol at 30.0 °C under hydrogen at one atmospheric pressure, as reported in Ref. 17. The catalyst dispersion (20 cm^3, total metal = 2×10^{-6} mol) was injected into a 50-cm^3 flask. An ethanol solution (1.0 cm^3) containing 0.2 mmol of a substrate (nitrobenzene or its derivatives) was added, and the progress of hydrogenation was followed by hydrogen uptake with a temperature-controlled gas burette. The initial rate was determined by the initial slope of hydrogen uptake and was used for the evaluation of catalytic activity in this paper. The hydrogenation products were analyzed with a Shimadzu GC-14B capillary gas chromatography using a 25 m×0.25 mmϕ WCOT fused silica capillary column.

Quantum Mechanical Analysis. Molecular property calculations of the substrate were carried out with the Gaussian 98 software package.[55] The geometry of each molecule was completely optimized at the density functional theory (DFT) level by analytic gradient techniques. A density functional theory (DFT) variant B3LYP with a standard basis set of 6-31+G(d,p) was performed, producing energy levels of the orbitals of each molecule.

Results and Discussion

Hydrogenation of Various Nitroaromatics to Aromatic Amines by Ni/Pd Bimetallic Nanoclusters. Colloidal dispersions of Ni/Pd bimetallic nanoclusters were prepared by glycol reduction at high temperature in the presence of poly(*N*-vinyl-2-pyrrolidone) (PVP), which appeared as clear dark brown solutions and had a good air-resisting property. They are stable for months under N_2 at room temperature. Especially, very dilute (0.1 mM) colloidal dispersions of the bimetallic nanoclusters, made for the use of catalysis, showed no precipitates nor inferiority in catalytic activities even after kept in the air for half a year, being quite comparable to the monometallic Pd clusters. The high stability may be attributed to the special structure of nanoclusters involving Ni–Pd bonds,[56] the complete surrounding of nanoclusters by polymers, and keeping nanoclusters in glycol solution, i.e., reductive atmosphere.[57] These Ni/Pd particles are considerably well-dispersed and uniform in size ranging from 1.2 to 2.5 nm (standard deviations range from 0.27 to 0.37 nm).[16,17] Structural analysis work of the Ni/Pd nanoclusters by XRD, EXAFS, and XPS has further shown the alloy structure in each particle with Ni at the zerovalent state.[16,17] Currently, they are applied for the catalysis of hydrogenation of various

nitroaromatics. During the reaction, the mixtures remained homogeneous without any precipitates of metal particles.

The hydrogenation of nitrobenzene is currently carried out over Pt- or Cu-based catalysts in industrial processes, during which high-temperature and high-pressure are indispensable. By the use of Ni/Pd bimetallic nanoclusters, however, the above reaction can be realized under a much milder condition, i.e., 30 °C and 1 atmosphere. Figure 1 compares the hydrogen uptake during the hydrogenation of *p*-nitroanisole, methyl *p*-nitrobenzoate, and nitrobenzene catalyzed by Ni/Pd(1/4) nanoclusters. The hydrogen uptake starts immediately after the addition of the substrates and increases linearly. Then, the hydrogen uptake suddenly ceases at three times the molar amounts of the substrates charged. The curves illustrate that the bimetallic nanocluster catalyst has both high activity and selectivity. Noticeably, the hydrogen uptake rate for *p*-nitroanisole is slower than that of nitrobenzene, and the latter is slower than that of methyl *p*-nitrobenzoate. In fact, product analysis by gas chromatography has proved that the substrates, such as *p*-nitroanisole, methyl *p*-nitrobenzoate, and nitrobenzene, have been totally transformed to the reduction products of *p*-aminoanisole, methyl *p*-aminobenzoate, and aniline, respectively. In the parallel experiments with alternative substrates including substituents like $-CH_3$, –CN, –Cl, and –Br, we observed that the Ni/Pd bimetallic nanoclusters are capable of reducing the nitro groups completely to amino groups in a similarly facile manner.

In particular, the substrate containing the *p*-cyano group shows its unique second step reduction occurring at the cyano group. Figure 2 shows the temporal uptake of hydrogen during the hydrogenation of *p*-nitrobenzonitrile catalyzed by Ni/Pd(1/4) nanoclusters. The hydrogen uptake is also initiated immediately after the addition of the substrate and increases linearly. Then, it reaches a plateau, after which

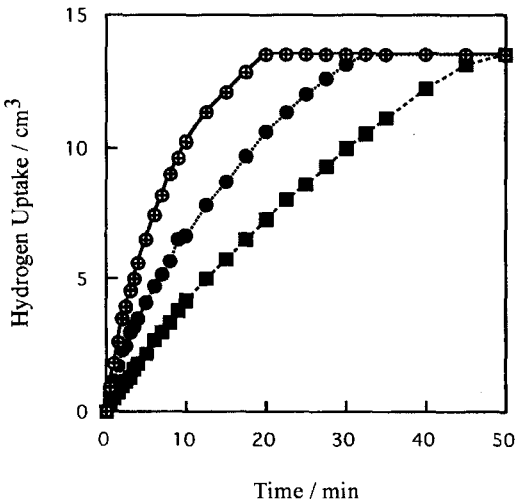

Fig. 1. Time course of hydrogen uptake of *p*-nitroanisole (■), nitrobenzene (●), and methyl *p*-nitrobenzoate (⊕) by bimetallic Ni/Pd(1/4) nanoclusters. [substrate] = 9.52 mM, [Ni/Pd nanocluster catalysts] = 0.095 mM, solvent: 21 cm^3 ethanol, at 30 °C, $p(H_2)$ = 1 atm.

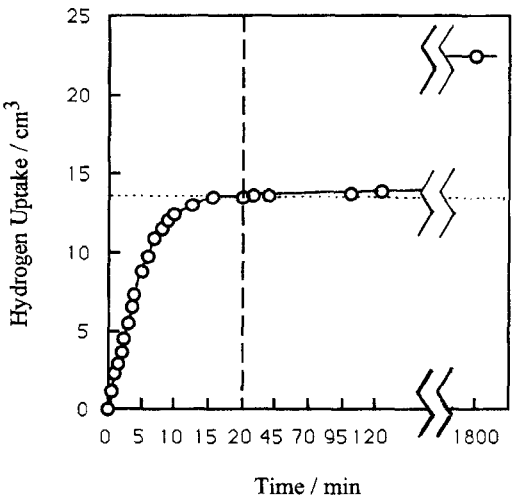

Fig. 2. Time course of hydrogen uptake of *p*-nitrobenzonitrile by bimetallic Ni/Pd(1/4) nanoclusters. Reaction conditions are the same as those in Fig. 1. Note that the scale of the abscissa before and after t = 20 min are different.

the hydrogen uptake continues to increase very slowly. The plateau represents three times the molar amounts of the substrate charged. Gas chromatographic analysis identified this plateau corresponding to the formation of the first step product, *p*-aminobenzonitrile, which was subsequently converted to the final product *p*-aminobenzylamine as confirmed by gas chromatography. This is shown in the slow rise after the plateau in Fig. 2.

Figure 3 shows the reaction profile of hydrogenation of *p*-nitrobenzonitrile by bimetallic Ni/Pd(1/4) nanoclusters. As the concentration of the substrate *p*-nitrobenzonitrile smoothly decreases with time, the final hydrogenation product *p*-aminobenzylamine, increases very slowly but steadily with time (t > 20 min). However, the in situ sampling

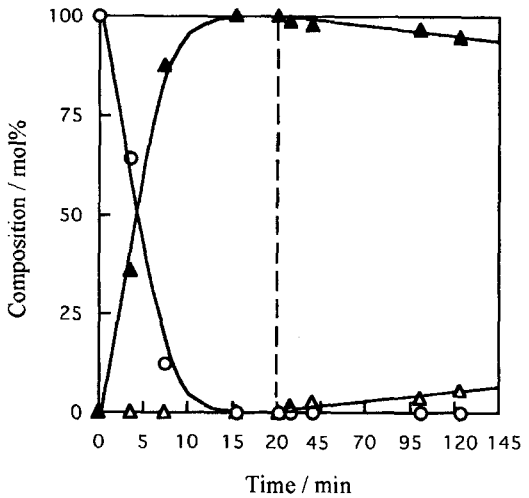

Fig. 3. Reaction profile of hydrogenation of *p*-nitrobenzonitrile by bimetallic Ni/Pd(1/4) nanoclusters. Reaction conditions are the same as those in Fig. 1. Note that the scales of the abscissa before and after t = 20 min are different. *p*-nitrobenzonitrile: ○, *p*-aminobenzonitrile: ▲, *p*-aminobenzylamine: △.

analysis shows that during the course of the reaction, apart from the substrate and final product, the first step reduction product species *p*-aminobenzonitrile is clearly observed in gas chromatography, which increases its concentration, then eventually decreases. The clear-cut reaction profile for the formation of *p*-aminobenzonitrile indicates that reduction of the nitro group has a lower energy barrier than that of the cyano group by this unique type of catalyst. The conversion of the cyano group to the aminomethyl group ($-CH_2NH_2$) occurs after the conversion of the nitro group to the amino group. It is concluded that the hydrogenation of the cyano group is only activated after the formation of an amino group at the *para*-position. It is obvious that selective hydrogenation of the nitro group in *p*-nitrobenzonitrile can be controlled at the first reaction step.

As for the substrates containing a *para*-halogen substituent, it is found that during the reduction of the nitro group the substrates undergo an interesting dehalogenation reaction, generating anilines as the final products. Although the mechanism of the coupled reactions of halogenated nitrobenzenes is a little complicated, its potential value is certainly remarkable in the dehalogenation of aromatic pollutants, as such colloidal particles may have some applications for dehalogenation of the halogenated aromatic compounds that are often listed as most hazardous organic pollutants.

Nanoclusters Having the Compositions with the Maximum Activity. Figure 4 shows the relationship between the catalytic activity and the metal composition of bimetallic Ni/Pd nanoclusters during the hydrogenation of nitrobenzene and its derivatives with electron-donating substituents, i.e., *p*-nitroanisole and *p*-nitrotoluene. It should be kept in mind that palladium is known to be a good catalyst for hydrogenation of a nitro group while nickel has very low activity.

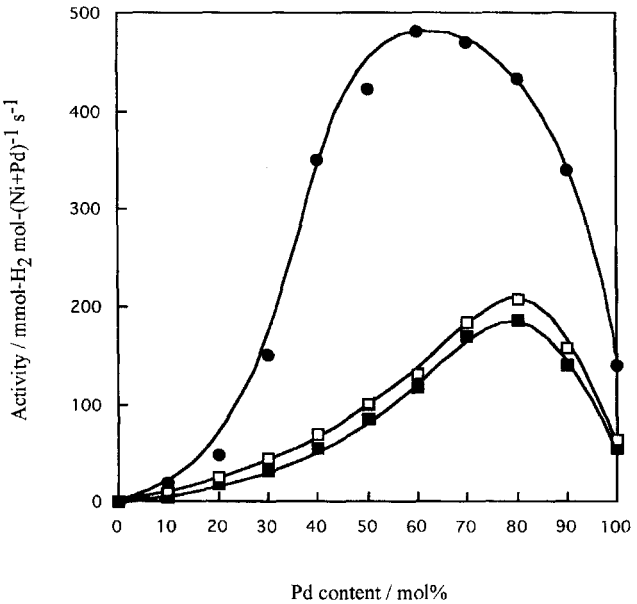

Fig. 4. Dependence of the catalytic activity of (■) *p*-nitroanisole, (□) *p*-nitrotoluene, and (●) nitrobenzene on the composition of Ni/Pd nanoclusters. Reaction conditions are the same as those in Fig. 1.

Colloidal dispersions of bimetallic Ni/Pd nanoclusters, especially those with a palladium content ranging from 40 to 90%, show much higher catalytic activity than both Ni and Pd monometallic nanoclusters. It has also been proved by our experiments that, commercial Raney Ni and Pd black catalysts show little activity for the same reaction. In particular, Ni/Pd(2/3) nanoclusters show the highest activity for nitrobenzene, ca. 3.5 times the value of monometallic Pd nanoclusters. Mixtures of colloidal dispersions of monometallic palladium and monometallic nickel nanoclusters, however, exhibit quite low activity. This clearly corroborates the conclusions that colloidal dispersions of bimetallic Ni/Pd nanoclusters are not mixtures of the corresponding monometallic nanoclusters, but rather each nanocluster particle contains both palladium and nickel atoms, forming a kind of an "alloy" structure, in accord with our previous results from EXAFS studies.[17] The interaction between palladium and nickel in a nanocluster particle could affect the catalytic activity.

Figure 4 also illustrates that the Ni/Pd(1/4) nanoclusters show the highest activity for *p*-nitroanisole and *p*-nitrotoluene, unlike the situation for nitrobenzene. It seems that introduction of a substituent on the *para* position affects the preference of close approaching of the substrate ring to the metal surface due to steric hindrance during the hydrogenation. The difference in the reaction activity between *p*-nitrotoluene and *p*-nitroanisole is small throughout the whole composition range, although the activity of *p*-nitrotoluene is considered to be higher than that of *p*-nitroanisole based on the electron-donating ability of the substituents. Both substrates have considerably lower activities than nitrobenzene. The underlying reason that *p*-nitrotoluene has a poor activity as low as *p*-nitroanisole may be attributed to the stiff bond between the methyl group and the benzene ring in *p*-nitrotoluene, preventing it from approaching closely to the metal surface due to the presence of a steric hindrance of the methyl group. In *p*-nitroanisole, the oxygen atom provides a bent C–O-ring bond, allowing the ring to approach the metal surface relatively closely.

Figure 5 compares the relationship between catalytic activity and the metal composition of bimetallic Ni/Pd nanoclusters during the hydrogenation of nitrobenzene and its derivatives with electron-withdrawing substituents, i.e., *p*-nitrobenzonitrile and methyl *p*-nitrobenzoate catalyzed by Ni/Pd(1/4) nanoclusters. The activity for *p*-nitrobenzonitrile only includes the conversion to *p*-aminobenzonitrile here. Again the Ni/Pd(1/4) nanoclusters show the highest activity for *p*-nitrobenzonitrile and methyl *p*-nitrobenzoate, which is even higher than monometallic Pd metal. It is obvious that the reaction rate for *p*-nitrobenzonitrile is faster than that for methyl *p*-nitrobenzoate throughout the whole composition range.

Figure 6 compares the relationship between catalytic activity and the metal composition of bimetallic Ni/Pd nanoclusters during the hydrogenation of nitrobenzene and 1-nitronaphthalene. The Ni/Pd(1/4) nanoclusters also show the highest activity for 1-nitronaphthalene. It appears that the large fused ring of naphthalene also affects the preference of

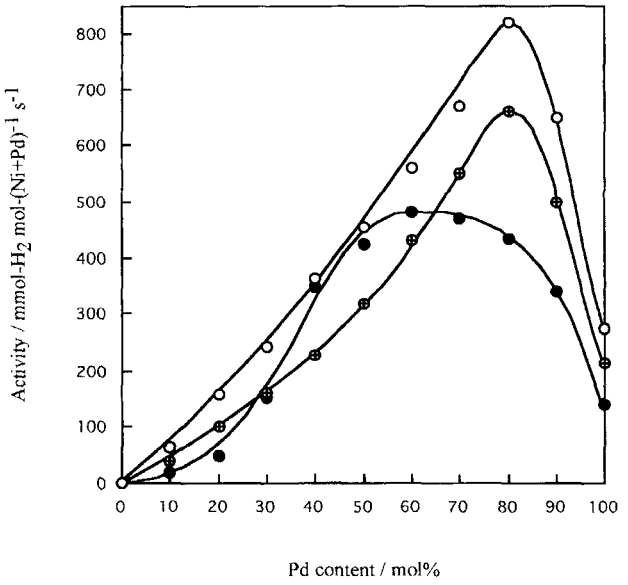

Fig. 5. Dependence of the catalytic activity of (○) *p*-nitrobenzonitrile, (⊕) methyl *p*-nitrobenzoate, and (●) nitrobenzene on the composition of Ni/Pd nanoclusters. Reaction conditions are the same as those in Fig. 1.

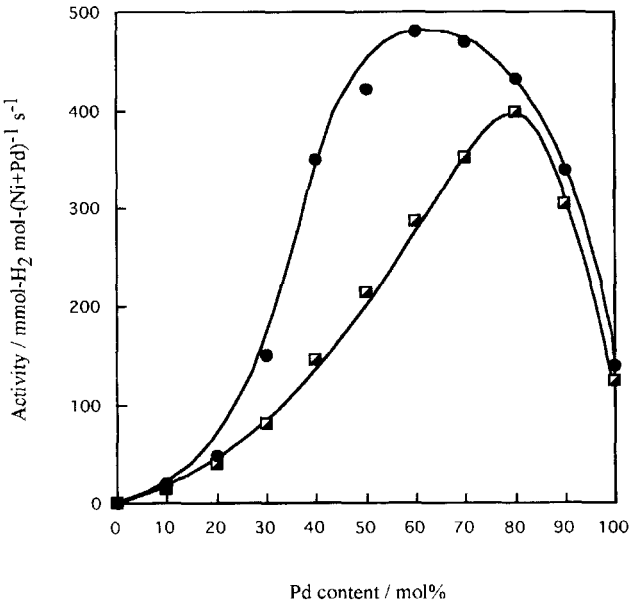

Fig. 6. Dependence of the catalytic activity of (◪) 1-nitronaphthalene and (●) nitrobenzene on the composition of Ni/Pd nanoclusters. Reaction conditions are the same as those in Fig. 1.

close approaching of the substrate ring to the metal surface. Such steric hindrance may lead to the decrease of the activity of 1-nitronaphthalene, when compared with nitrobenzene.

To examine the influence of the surface area of the catalyst, the catalytic activity was normalized by the total surface area of the particles, which was calculated using the average diameter of the nanocluster particles measured by TEM.[17] The dependence of the normalized activity for the substrates containing electron-donating groups, that for the substrates containing electron-withdrawing groups, and that for 1-naphthalene on the metal compositions, show similar shapes to those of the apparent activity illustrated in Figs. 4, 5, and 6 respectively. This fact indicates that the higher activity of the bimetallic nanoclusters in the region near Ni/Pd 1/4 ratio than the monometallic nanoclusters is not due to the surface area of those particles, nor due to the particle size variations, but due to the special structure of the alloy particles. Only a ligand and/or *ensemble* effect may account for the activity dependence on the metal compositions in these bimetallic nanoclusters.[44] In general, palladium has a relatively high catalytic activity, while nickel has a low activity. Nevertheless, Ni/Pd bimetallic nanoclusters hold catalytic activity higher than either of these monometallic nanoclusters for the hydrogenation of nitrobenzenes. We can see that the Ni/Pd bimetallic system is not composed of the bimetallic nanoclusters with the special Pd-shell Ni-core structure, but the nanoclusters with Ni and Pd atoms coexisting on the surface.

The surface segregation of palladium has been suggested by EXAFS analysis.[17] It is also found that the total coordination number around nickel is much larger than that around palladium, suggesting that palladium atoms are located preferentially on the surface. So the model where both elements are mostly randomly located in a particle, forming an alloy with a little richness of palladium near the surface, can be proposed for this novel Ni/Pd bimetallic nanoclusters. The adjacent noble metal palladium in this structure may prevent nickel from oxidation and the neighboring nickel can provide an *ensemble* effect upon the catalysis of the noble metal, thereby controlling the maximum activity of the substrates through alloy compositions.

Dependence of the Substrate Reactivity on the Substituent. The maximum catalytic activities vary in the following order from high to low: *p*-nitrobenzonitrile > methyl *p*-nitrobenzoate > nitrobenzene > 1-nitronaphthalene > *p*-nitrotoluene > *p*-nitroanisole. The electron-withdrawing and electron-donating effect of the substituent may play an important role in generating this result. The present result can be explained by an empirical substitution effect, which can be quantified by the Hammett constant.

When Ni/Pd(1/4) bimetallic nanoclusters are used as the catalyst, an approximately linear relationship is observed between the hydrogenation rate and the Hammett constant (σ_p value) of the substituents (correlation coefficient = 0.998) as shown in Fig. 7.[58] For catalysts with other composition ratios, similar relationships were also observed. It is concluded that the electronic effect of the substituents controls the electron densities, and hence, the reactivity of nitro group at the *para*-position. The reactivity is mainly governed by the electronic effect, but a certain degree of steric hindrance has very probably led to the deviation of the linearity of the correlation in Fig. 7. The latter effect may account for the low activity of *p*-nitrotoluene.

The slope of the Hammett relationship shown in Fig. 7 may suggest that the hydrogenation of nitrobenzene derivatives is aided by electron withdrawal from the benzene ring. In other words, the rate determination step of the reaction is nucleophilic attack by a nucleophile, which is probably hy-

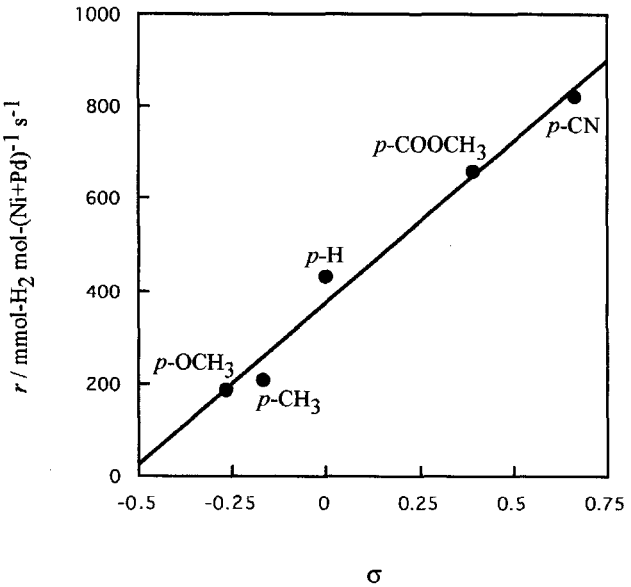

Fig. 7. Relationship between Hammett constant σ and the catalytic activity r of nitrobenzene derivatives catalyzed by Ni/Pd(1/4) nanoclusters.

dride (H^-) produced by dissociative adsorption of hydrogen molecule on the catalyst surface. This idea is also suggested by the molecular orbital consideration, as shown in the next paragraph.

In order to understand the substituent effect by using quantum chemical approaches, frontier orbitals of the derivatives, i.e., the energy levels of highest occupied molecular orbital (HOMO) and lowest unoccupied molecular orbital (LUMO), are calculated. These quantum-chemical characteristics can be used in a similar way as Hammett constants, as they all describe intrinsic properties of the nitrobenzene derivatives before being perturbed by adsorption on metals, and can be calculated by a high-precision density functional theory method. The currently favored approach or the density functional theory (DFT)[59] has the advantage of including the effects of electron correlation in a computationally efficient manner, unlike the *ab initio* Hartree–Fock method.

As seen in Table 1, different substituents have a progressive variation in the energy levels of the LUMO and HOMO, which in turn seem to have a correlation with the hydrogenation rates. Adsorption of the substrates inevitably brings about interactions of the alloy metal's valence electrons with either the HOMO of the substrates or the LUMO of the adsorbate molecule (back donation). Although a detailed calculation of the catalyst system including both metal atoms may be more illustrative to understand the adsorption interactions here, such a calculation is too formidable, because the complicated details of the specific adsorption geometries of a nitro compound on the metal alloys and in the absence and/or presence of a hydrogen molecule will be included. We simplify the structural considerations without introducing the metals, as the metal surface is believed to exert an equal effect on all of the substrates. But obviously, a better reactivity is brought about by a more favorable interaction between the frontier orbitals of the substrates and metal valence level, and such favorably recombined orbitals result in more reactivity to accept electrons from the coadsorbed hydrogens for the reduction.

Table 1. Energy Levels of HOMO and LUMO Orbitals Nitrobenzene Derivatives with Different Substituents at *para*-Position

Substituent	HOMO (eV)	LUMO (eV)
CH_3O–	−0.26042	−0.09763
CH_3–	−0.28126	−0.10268
H–	−0.29022	−0.10736
CH_3OOC–	−0.29703	−0.12055
–CN	−0.30917	−0.13252

Figure 8 shows the relationship between LUMO energy and the catalytic activity of nitrobenzene derivatives by Ni/Pd(1/4) nanocluster (correlation coefficient 0.981). The correlation between HOMO energy and the catalytic activity of nitrobenzene derivatives by Ni/Pd(1/4) nanocluster (correlation coefficient 0.915) is worse than in the case of LUMO energy levels. Hence, it may be concluded that the rate-determining step is the attack of the hydride anion toward the LUMO orbitals of the nitro groups and the reaction has strong nucleophilic character. The LUMO coefficients (Table 2) show that all the LUMO orbitals of those five substrates have large contributions from the nitro group (from N $2p_z$ orbital, and O $2p_z$ orbital). The nitro group is indeed involved in the LUMO orbitals of the whole molecule. Another result from the calculation is that the $-NO_2$ group is comprised of N–O antibonding in the LUMO, in which the p_z orbital of the N atom is in the opposite direction to the p_z orbital of the O atom. These features can be clearly seen in Fig. 9, which shows the HOMO and LUMO orbital diagrams of nitrobenzene.

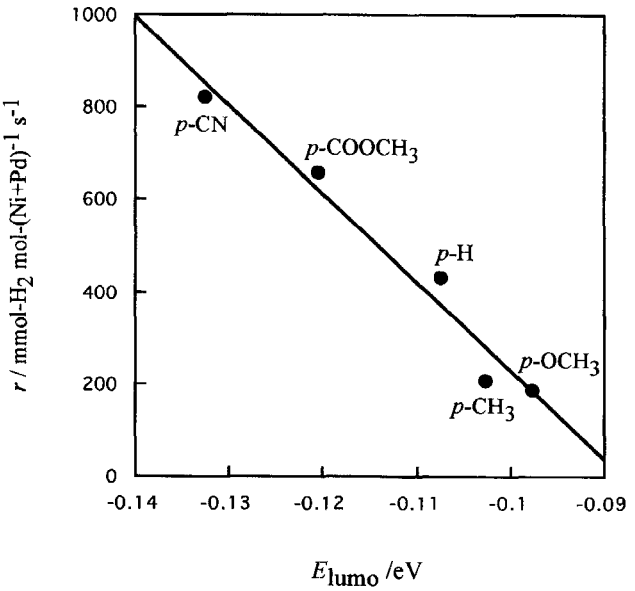

Fig. 8. Relationship between LUMO energy E_{lumo} and the catalytic activity r of nitrobenzene derivatives catalyzed by Ni/Pd(1/4) nanoclusters.

Table 2. Molecular Orbital Coefficients of the LUMO Orbital in the $-NO_2$ Moiety of Nitrobenzene Derivatives with Different Substituents at *para*-Position

Substituent	$N2p_z$	$O(1)2p_z$	$O(2)2p_z$
CH_3O-	+0.42634	−0.31924	−0.32252
CH_3-	+0.41793	−0.32067	−0.31939
H–	+0.41512	−0.32061	−0.32061
CH_3OOC-	+0.35868	−0.29304	−0.29260
–CN	+0.35634	−0.29393	−0.29393

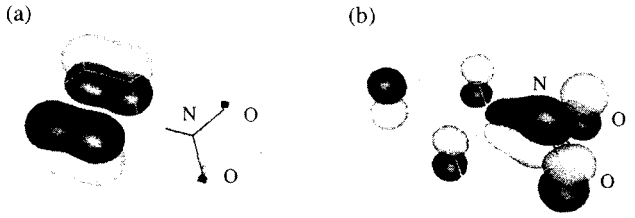

Fig. 9. (a) HOMO and (b) LUMO orbital diagrams of nitrobenzene.

The catalysis results indicate that the polymer-protected Ni/Pd bimetallic nanoclusters with palladium mole ratio in a certain intermediate composition range exhibit higher catalytic activity than either monometallic nickel or palladium nanoclusters and that the maximum catalytic activity was observed at a certain Ni/Pd ratio. Unlike the case of hydrogenation of nitrobenzene, the highest catalytic activity exists at Ni/Pd bimetallic nanoclusters with mole ratio of 1/4 in the hydrogenation of nitrobenzene derivatives, rather than 2/3 in that of nitrobenzene. We consider the following factors in interpreting the observations here. Thus, two opposite effects for the hydrogenation of nitrobenzene may be predicted to occur by the joining of nickel into palladium to form an alloy structure: (1) The first effect is based on the catalytic activity of palladium hydride (Pd–H), where it will decrease with the increase of nickel contents. (2) The other effect originates from the interaction between the catalyst surface, especially the nickel surface, and the substrate. The nickel surface makes it easier to form a charge-transfer complex with the benzene ring of the substrates than the palladium surface, so that the more nickel atoms are in the alloy particle, the stronger the interaction. A combined result of the above two effects has led to the maximum activity in the intermediate composition. Although the above considerations are still speculative, the result that only nitrobenzene shows the maximum at 2/3 ratio, unlike all other derivatives at 1/4 ratio, could suggest the existence of the steric effect of the *p*-substituent.

Conclusions

The catalytic performance of a novel type of nanometer-sized alloy particles, namely, the late transition metal-noble metal bimetallic nanoclusters, is described for the hydrogenation of various nitrobenzene derivatives. Although a bimetallic nanocluster with a molar ratio of Ni : Pd = 2/3 was the most active catalyst for the hydrogenation of nitrobenzene, the nanoclusters with the molar ratio of Ni : Pd = 1/4 were the most active catalyst for the hydrogenation of its derivatives. The magnitude of the maximum catalytic activities for different substrates varied in an increasing order: $CH_3O- < CH_3- < H- < CH_3OOC- < -CN$. They are proved to be efficient catalysts for hydrogenation of a nitro group to an amino group; interesting catalytic phenomena attributable to substituent electronic effect and steric hindrance effect have been observed. Both nickel and palladium play an important role in the catalytic behavior of this bimetallic nanocluster catalyst. A kind of 'mostly random with a little palladium richness on the cluster surface' model structure other than hitherto often reported 'core-shell' model structure for noble metal bimetallic nanoclusters can account for the hydrogenation reactions reported here.

This work has been supported by a Grant-in-Aid for Scientific Research in Priority Area "New Polymers and Their Nano-Organized System" (No. 08246101, to N.T.) from the Ministry of Education, Science, Sports and Culture.

References

1 J. A. A. Perenboom, P. Wyder, and F. Meier, *Phys. Rep.*, **78**, 173 (1981).
2 W. P. Halperin, *Rev. Mod. Phys.*, **58**, 533 (1986).
3 M. T. Reetz and W. Helbig, *J. Am. Chem. Soc.*, **116**, 7410 (1994).
4 N. Toshima, in "Fine Particles Science and Technology—From Micro to Nanoparticles," ed by E. Pelizzetti, Kluwer, Dordrecht (1996), pp. 371—383.
5 N. Toshima, *J. Macromol. Sci.-Chem.*, **A27**, 1225 (1990).
6 N. Toshima, *Macromol. Symp.*, **105**, 111 (1996).
7 H. Hirai and N. Toshima, "Tailored Metal Catalysts," ed by Y. Iwasawa, D. Reidel Pub., Dordrecht (1986), p. 87.
8 H. Hirai and N. Toshima, "Polymeric Materials Encyclopedia," ed by J. C. Salamone, CRC Press, Boca Raton (1996), Vol. 2/C, pp. 1310—1316.
9 G. Schmid, *Chem. Rev.*, **92**, 1709 (1992).
10 M. T. Reetz and S. A. Quaiser, *Angew. Chem., Int. Ed. Engl.*, **34**, 2240 (1995).
11 N. Toshima, K. Kushihashi, T. Yonezawa, and H. Hirai, *Chem. Lett.*, **1989**, 1769.
12 N.Toshima, M. Harada, T. Yamazaki, and K. Asakura, *J. Phys. Chem.*, **96**, 9927 (1992).
13 T. Yonezawa and N. Toshima, *J. Mol. Catal.*, **83**, 167 (1993).
14 M. Harada, K. Asakura, and N. Toshima, *J. Phys. Chem.*, **98**, 2653 (1994).
15 N. Toshima and Y. Wang, *Langmuir*, **10**, 4574 (1994).
16 N. Toshima and P. Lu, *Chem. Lett.*, **1996**, 729.
17 P. Lu, T. Teranishi, K. Asakura, M. Miyake, and N. Toshima, *J. Phys. Chem. B*, **103**, 9673 (1999).
18 L. Petrov, K. Kumbilieva, and N. Kirkov, *Appl. Catal.*, **59**, 31 (1990).
19 M. Wojciechowska, S. Lomnicki, J. Bartoszewicz, and J. Goslar, *J. Chem. Soc., Faraday Trans.*, **91**, 2207 (1995).
20 X. M. Fang, S. L. Yao, Z. Qing, and F. Y. Li, *Appl. Catal. A-General*, **161**, 129 (1997).
21 U. Kurschner, H. Ehwald, and G. Alscher, *Catal. Lett.*, **34**, 191 (1995).
22 S. Yada, T. Sasaki, M. Hiyamizu, and Y. Takagi, *Bull. Chem.*

Soc. Jpn., **69**, 2383 (1996).
23 D. J. Collins, R. P. Schneider, M. C. Wolf, and B. H. Davis, *J. Mol. Catal.*, **62**, 57 (1990).
24 J. Peureux, M. Torres, H. Mozzanega, A. Giroirfendler, and J. A. Dalmon, *Catal. Today*, **25**, 409 (1995).
25 C. P. Li, Y. W. Chen, and W. J. Wang, *Appl. Catal. A-General*, **119**, 185 (1994).
26 G. C. Torres, E. L. Jablonski, G. T. Baronetti, A. A. Castro, S. R. deMiguel, O. A. Scelza, M. D. Blanco, M. A. P. Jimenez, and J. L. G. Fierro, *Appl. Catal. A-General*, **161**, 213 (1997).
27 E. Baumgarten, A. Fiebes, and A. Stumpe, *React. Functio. Polym.*, **33**, 71 (1997).
28 P. C. Selvaraj and V. Mahadevan, *J. Polym. Sci., Part A-Polym. Chem.*, **35**, 105 (1997).
29 J. Gao, F. D. Wang, S. J. Liao, and D. R. Yu, *React. Kinet. Catal. Lett.*, **64**, 351 (1998).
30 Y. An, M. Suzuki, T. Koyama, K. Hanabusa, H. Shirai, M. Huang, and Y. Jiang, *Polym. Adv. Technol.*, **7**, 652 (1996).
31 A. Tijani, B. Coq, and F. Figueras, *Appl. Catal.*, **76**, 255 (1991).
32 D. R. Patel, M. K. Dalal, and R. N. Ram, *J. Mol. Catal. A-Chem.*, **109**, 141 (1996).
33 J. J. Jin, G. C. Chen, M. Y. Huang, and Y. Y. Jiang, *React. Polym.*, **23**, 95 (1994).
34 Z. K. Yu, S. J. Liao, Y. Xu, B. Yang, and D. R. Yu, *J. Mol. Catal. A-Chem.*, **120**, 247 (1997).
35 D. R. Patel and R. N. Ram, *J. Mol. Catal. A-Chem.*, **130**, 57 (1998).
36 Z. Bodnar, T. Mallat, and A. Baiker, *Catal. Lett.*, **26**, 61 (1994).
37 G. M. Schwab, *Discuss. Faraday Soc.*, **8**, 166 (1950).
38 D. A. Dowden, *J. Chem. Soc.*, **1950**, 242.
39 D. A. Dowden and P. Reynolds, *Discuss. Faraday Soc.*, **8**, 184 (1950).
40 V. Ponec, in "Advances in Catalysis," ed by D. D. Eley, H. Pines, and P. B. Weisz, Academic Press, San Diego (1983), Vol. 32, p. 149.
41 V. Ponec, *Catal. Rev. Sci. Eng.*, **11**, 41 (1975).
42 J. K. Clarke, *Chem. Rev.*, **75**, 291 (1975).
43 J. H. Sinfelt, *Acc. Chem. Res.*, **10**, 15 (1977).
44 J. H. Sinfelt, "Bimetallic Catalysts," Wiley, New York (1983).
45 W. M. H. Sachtler and R. A. van Santen, in "Advances in Catalysis," ed by D. D. Eley, H. Pines, and P. B. Weisz, Academic Press, New York (1977), Vol. 26, p. 69.
46 J. J. Burton and R. L. Garten, "Advanced Materials in Catalysis," Academic Press, New York (1977).
47 K. I. Chio and M. A. Vannice, *J. Catal.*, **131**, 36 (1991).
48 W. M. H. Sachtler and R. A. van Santen, *Adv. Catal.*, **26**, 69 (1977).
49 J. S. Feeley, A. Y. Stakheer, F. A. P. Cavalcanti, and W. M. H. Sachtler, *J. Catal.*, **136**, 182 (1992).
50 J. H. Sinfelt, Y. L. Lam, J. A. Cusumano, and A. E. Barnett, *J. Catal.*, **42**, 227 (1976).
51 G. R. Sheffer and T. S. King, *J. Catal.*, **116**, 488 (1989).
52 J. A. Brown, A. Bourtzutschky, N. Homs, and A. T. Bell, *J. Catal.*, **124**, 73 (1990).
53 J. S. Pizey, "Synthetic Reagents," Ellis Horwood, Chichester (1974), Vol. 2, pp. 175—311.
54 Chemical Society of Japan, "Kagaku Binran," Maruzen, Tokyo (1984), p. II-718.
55 M. J. Frisch, G. W. Trucks, H. B. Schlegel, G. E. Scuseria, M. A. Robb, J. R. Cheeseman, V. G. Zakrzewski, J. A. Montgomery, R. E. Stratmann, J. C. Burant, S. Dapprich, J. M. Millam, A. D. Daniels, K. N. Kudin, M. C. Strain, O. Farkas, J. Tomasi, V. Barone, M. Cossi, R. Cammi, B. Mennucci, C. Pomelli, C. Adamo, S. Clifford, J. Ochterski, G. A. Petersson, P. Y. Ayala, Q. Cui, K. Morokuma, D. K. Malick, A. D. Rabuck, K. Raghavachari, J. B. Foresman, J. Cioslowski, J. V. Ortiz, B. B. Stefanov, G. Liu, A. Liashenko, P. Piskorz, I. Komaromi, R. Gomperts, R. L. Martin, D. J. Fox, T. Keith, M. A. Al-Laham, C. Y. Peng, A. Nanayakkara, C. Gonzalez, M. Challacombe, P. M. W. Gill, B. G. Johnson, W. Chen, M. W. Wong, J. L. Andres, M. Head-Gordon, E. S. Replogle, and J. A. Pople, "Gaussian 98 (Revision A.1)," Gaussian, Inc., Pittsburgh, PA (1998).
56 E. K. Hlil, R. Baudoing-Savors, B. Moraweck, and A. J. Renouprez, *J. Phys. Chem.*, **100**, 3102 (1996).
57 T. Yonezawa and N. Toshima, *J. Chem. Soc., Faraday Trans.*, **91**, 4111 (1995).
58 L. P. Hammett, *Chem. Revs.*, **17**, 225 (1935); "Physical Organic Chemistry," 2nd ed, McGraw-Hill, New York (1970).
59 R. G. Parr and W. Yang, "Density Functional Theory of Atoms and Molecules," Oxford University Press, New York (1989).